Article

Theoretical Studies of Conjugation Effects on Excited State Intramolecular Hydrogen-Atom Transfer Reactions in Model Systems

Carlos R. Baiz, and Barry D. Dunietz

J. Phys. Chem. A, **2007**, 111 (40), 10139-10143• DOI: 10.1021/jp074290i • Publication Date (Web): 19 September 2007

Theoretical Studies of Conjugation Effects on Excited State Intramolecular Hydrogen-Atom Transfer Reactions in Model Systems

Carlos R. Baiz and Barry D. Dunietz*

Department of Chemistry, University of Michigan, Ann Arbor, Michigan 48109-1055

Received: June 4, 2007; In Final Form: August 6, 2007

Intramolecular hydrogen-atom transfer dependence on electronic conjugation of curcumin and related molecular models in the ground state and $^1\pi\pi^*$ excited state are computationally studied at the first-principles electronic structure level. The larger, more conjugated, systems exhibit a lower reaction barrier in the ground state but a higher barrier in the excited state. This is associated with a smaller increase in the conjugation upon excitation in the larger systems. Our studies provide a detailed description and analysis of these energy trends as well as an insight into the physical nature of the intramolecular hydrogen-atom transfer reactions.

I. Introduction

Intramolecular hydrogen-atom transfer (IHT) reactions are of central importance in a variety of chemical and biological processes. These IHT reactions have been thoroughly studied experimentally in the ground and excited states[1−10] and theoretically using electronic structure methods.[11−19] Some of these theoretical studies have been revealing unexpected behaviors related to electronic structure changes induced upon excitation.[13,20]

The effect of the backbone conjugation on the potential energy surface of the ground and excited state IHT reactions is investigated. This is of high significance as high-level theoretical studies use smaller model systems to mimic IHT reactions in larger systems with an extended conjugated backbone. In this report we use a series of model molecules with increasing size of the coupled backbone to obtain physical insight into the IHT reaction and the effect of the backbone conjugation on excited state reaction energy barriers.

We extend our set of model systems to include Curcumin (model **IV** in Figure 1), a natural compound derived from *Curcuma longa* known for its antioxidant and anti-inflammatory properties.[21−23] Curcumin and several of its analogs[24] have also shown tumor inhibiting and anti-amyloidogenic properties and potential as a cure for Alzheimer's disease.[25,26] A photolysis study by Jovanovic et al. attributes the antioxidant mechanism of curcumin to intermolecular H-atom transfer in the diketo-form.[27] A recent *ab initio* study by Balasubramanian suggests that the enolic form of curcumin may be responsible for the inhibition of β-amyloid aggregation.[28] However, the nature of many biomolecular properties of curcumin remains unclear; therefore, it is important to investigate the structure and reactivity of this prolific medicinal agent.

Our main interest here, however, is to use the models considered to provide insight on the effect of increasing the coupled conjugated backbone in the excited state IHT process. Recently, with the advent of new ultrafast time-domain four-wave mixing spectroscopies,[29,30] it has become possible to directly observe hydrogen-bond dynamics in real time with femtosecond time resolution.[31] The rising interest in the use of ultrafast spectroscopy to study hydrogen transfer reactions has motivated several experiments. We expect that the present report will help to stimulate and assist to interpret new spectroscopic studies on rapid intramolecular hydrogen transfer reactions. This has also the potential to enhance the understanding of the remarkable properties of the curcumin molecule.

II. Computational Methods and Models

We defined a set of model molecules, where the backbone conjugation is varied as shown in Figure 1, to study the effects of conjugation on excited state IHT reaction barriers. We did not include in the set the smallest related system, malonaldehyde, because excited state studies of this system have been previously reported in the literature.[14,32−35] In addition, we have found that the IHT barrier of this small system differs by approximately 10 kJ mol^{-1} in the ground state from our next larger system (model **I**) whereas the difference in IHT barrier among our models **I**−**IV** is on the order of 2 kJ mol^{-1}. Therefore, malonaldehyde is inherently a different system and not an accurate model for the bigger molecules involving backbone conjugation.

Initial geometries for all models were obtained with the density functional theory (DFT) method using Becke's three -parameter B3 nonlocal exchange[36] and Lee−Yang−Parr's correlation functional (LYP)[37] with the 6-31G basis set. These ground state geometries were then further optimized with the spin-restricted Hartree−Fock and B3-LYP methods using two different basis sets 6-31G(d) and 6-31++G(d,p), to obtain the final ground state geometries. As previously reported, the planar enol geometry is lower in energy than the nonplanar diketo conformation.[38]

Excited state geometries were obtained by optimizing the corresponding ground state geometries employing the configuration interaction single-excitations (CIS) method,[39] where the spin-restricted Hartree−Fock is used as the reference ground state. The same basis sets employed in the ground state computations were used with the CIS method. Excited state geometries were optimized in the lowest singlet excited state corresponding to the $^1\pi\pi^*$ transition. This particular excited state was chosen because it is the only one of the lower energy states that exhibits a large transition dipole moment. The $^1\pi\pi^*$ transition in our model **IV** system is approximately 4.90 atomic units in the plane of the molecule, whereas, due to molecular

* Corresponding author. E-mail: bdunietz@umich.edu.

10.1021/jp074290i CCC: $37.00
Published on Web 09/19/2007

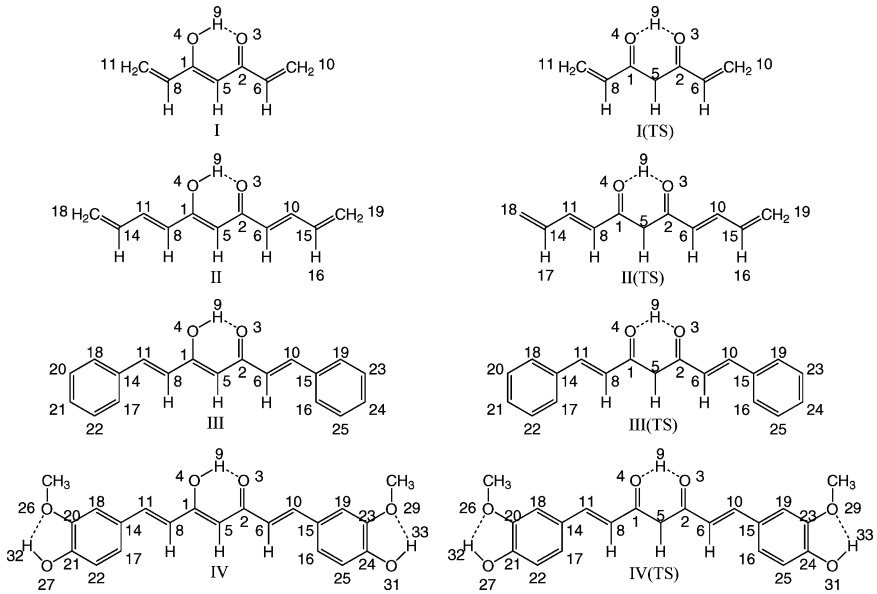

Figure 1. Molecular structures of the four model systems in their enol and transition state (TS) configurations.

symmetry, the transition dipole moments corresponding to the two lower energy $^3n\pi^*$ and $^3\pi\pi^*$ electronic transitions are exactly zero. Therefore, this state is likely the only (low) excited state experimentally accessible. Transition state (TS) geometries were obtained by minimizing along all coordinates except for the coordinate corresponding to the IHT reaction. The ground and excited state TS geometries exhibited one imaginary frequency corresponding to the motion of the hydrogen atom along the IHT reaction coordinate. All calculations were performed employing a pre-release version of Q-Chem 3.1 package of programs.[40] Density of states plots were obtained using our own code implementing a Green's function based formalism.[41]

The degree of conjugation was measured by a generalized nonconjugation index ξ defined by the difference in length between the longest and shortest carbon−carbon bonds. We focus the analysis of the degree of conjugation on the core of the system involving atoms C_1, C_2, C_5, C_6, and C_8, as shown in Figure 1. We also include in this evaluation the bonds of the core atoms to the α carbons (C_{11}, C_{10}). Therefore, electronic conjugation at this region is referred to as the core conjugation. The rest of the molecule, which is coupled to the core, is referred to as the backbone. The core conjugation is shown below to depend on the extent of the coupled conjugated backbone and to affect the energy barrier for the proton transfer reaction.

III. Results and Discussion

DFT calculations grossly underestimate hydrogen transfer barriers in the ground state. The B3LYP/6-31++G(d,p) method, when applied to model systems (**I**−**IV**), failed to predict an energy barrier. The obtained barriers, after adding the respective zero point vibrational energy (ZPVE) corrections, were on the order of −3 kJ mol^{-1}. This is attributed to an overestimation of electron correlation energy. Previous studies have shown that the computed IHT barrier is lowered when electron correlation is added perturbatively to ground state Hartree−Fock calculations,[13] and that DFT underestimates the ground state proton transfer barrier in $(FHF)^-$.[43] A recent molecular dynamics study suggests that this barrier completely vanishes in the $^1\pi\pi^*$ state.[20] However, it is important to point out that the overall decrease in ground state hydrogen-atom transfer barrier with increasing backbone conjugation, as discussed below, was predicted by the B3LYP method as well.

As previously reported,[42] the computed ground state IHT barriers are not strongly dependent on the choice of basis set. We have observed that the ground state IHT barriers predicted by the 6-31G(d) basis set are on average 5 kJ mol^{-1} higher than those predicted by the larger 6-31++G(d,p) basis set. As shown in Table 1, ground state IHT barriers are in the order of 18−20 and 23−26 kJ mol^{-1} as calculated with the 6-31++G(d,p), and 6-31G(d) basis sets, respectively. The excited state barriers are more dependent on the choice of basis set; we observe that, with the smaller basis set, the barrier at the excited electronic state for the small model (**I**) is lowered from 9.16 to 7.74 kJ mol^{-1}, but in the larger systems this is reversed and the energy barrier with the smaller 6-31G(d) basis set is increased from 12.03 to 15.97 kJ mol^{-1} in the case of curcumin (model **IV**).

One important observation is that at the ground electronic state the energy barrier is slightly lowered for the larger systems. The barrier decreases from 20.37 kJ mol^{-1} in model **I** to 18.22 kJ mol^{-1} in model **IV** as computed with the larger 6-31++G-(d,p) basis set. This reaction, as revealed by Mulliken charge analysis and comparison of the projected density of states plot of the enol to the identified TS, involves a charge transfer toward the system core. The core atoms are denoted in Figure 1 as C_1, C_2, O_3, O_4, C_5, and H_9, whereas the rest are considered the backbone. We find, for example, that for model **I** the sum of the Mulliken charges on the core atoms changes from −0.286 to −0.319 in the enol to the TS, respectively. In addition, the Mulliken analysis reveals that the hydrogen atom, H_9, becomes more positive in the transition state.

The hydrogen-atom transfer reaction coordinate, therefore, involves the charge transfer from the hydrogen atom and the backbone of the molecule to the atoms that compose the core, mainly 0_3 and 0_4. In addition, we also observe some geometrical relaxation of the core structure along the reaction coordinate as shown in Table 2. The data show that a decrease in the distance between the two oxygen atoms of 0.3 Å occurs as the system moves along the reaction coordinate from the equilibrium to the transition states.

TABLE 1: Ground and Excited State Total Electronic Energies (TE) in Atomic Units, Zero Point Vibrational Energies (ZPVE) in Atomic Units, and Corresponding IHT Barriers (ΔE) (kJ mol^{-1}) Calculated at the HF/6-31++G(d,p), HF/6-31G(d) and CIS/6-31++G(d,p), CIS/6-31G(d) Respective Levels of Theory

	ground			excited		
model	TE	ZPVE	ΔE	TE	ZPVE	ΔE
			6-31++G(d,p) Basis Set			
I	−419.4465919	0.1446018		−419.2619062	0.1409508	
I(TS)	−419.4337271	0.1394943	20.37[a]	−419.2546496	0.1371852	9.16
II	−573.2378096	0.2161481		−573.0721402	0.2151393	
II(TS)	−573.2254591	0.2111569	19.32	−573.0634643	0.2102980	10.07
III	−878.5836092	0.3182868		−878.4289042	0.3200015	
III(TS)	−878.5715504	0.3133785	18.77	−878.4190864	0.3147840	12.08
IV	−1256.0822355	0.3981039		−1255.9321556	0.3998218	
IV(TS)	−1256.0703868	0.3931940	18.22	−1255.9222742	0.3945215	12.03
			6-31G(d) Basis Set			
I	−419.4135300	0.1452233		−419.2219327	0.1406640	
I(TS)	−419.3985949	0.1401684	25.94[b]	−419.2147256	0.1364043	7.74
II	−573.1928294	0.2172652		−573.0212668	0.2137163	
II(TS)	−573.1784496	0.2121896	24.43	−573.0116190	0.2088430	12.54
III	−878.5248829	0.3197608		−878.3649958	0.3166390	
III(TS)	−878.5107351	0.3146820	23.81	−878.3538263	0.3116335	16.18
IV	−1255.9981824	0.4002234		−1255.8433575	0.3974330	
IV(TS)	−1255.9843119	0.3951509	23.10	−1255.8320505	0.3922107	15.97

[a] In good agreement with the previously reported value of 20.95 kJ mol^{-1}.[42] [b] In good agreement with the previously reported value of 26.30 kJ mol^{-1}.[42]

TABLE 2: Distances (R, Å) and Angles (A, Degrees) for Models I and IV Calculated with the HF/6-31++G(d,p) Method in the Ground State, S_o, and CIS/6-31++G(d,p) Method in the Excited $^1\pi\pi^*$ State

	S_o **I**(enol, TS)	$\pi\pi^*$ **I**(enol, TS)	S_o **IV**(enol, TS)	$\pi\pi^*$ **IV**(enol, TS)
$R(O_4-H_9)$	0.959, 1.185	0.976, 1.195	0.961, 1.184	0.966, 1.187
$R(O_3-H_9)$	1.795, 1.185	1.683, 1.195	1.769, 1.184	1.727, 1.187
$R(O_3-O_4)$	2.621, 2.320	2.559, 2.342	2.606, 2.321	2.587, 2.333
$R(C_1-C_5)$	1.355, 1.401	1.447, 1.440	1.358, 1.401	1.402, 1.417
$R(C_5-C_2)$	1.454, 1.401	1.434, 1.440	1.452, 1.401	1.433, 1.417
$R(C_1-O_4)$	1.316, 1.265	1.305, 1.227	1.318, 1.270	1.325, 1.285
$R(C_2-O_3)$	1.219, 1.265	1.248, 1.227	1.224, 1.270	1.242, 1.285
$A(C_1O_4H_9)$	109.3, 103.2	108.7, 103.8	108.8, 103.1	108.3, 103.2
$A(C_1C_5C_2)$	121.8, 116.8	122.3, 118.5	121.9, 117.2	122.2, 118.4

We now compare the different models in the ground state. A Mulliken charge population analysis reveals that the charge on the two oxygen atoms (O_3, O_4) decreases slightly from −0.706 in model **I(TS)** to −0.703 in model **IV(TS)** and that the charge separation between the two oxygens in the enol form decreases from 0.025 in model **I** to 0.005 in model **IV**. The charge on the hydrogen atom (H_9) also decreases from 0.490 in model **I(TS)** to 0.488 in model **IV(TS)**. Considering, as shown in Table 2, the corresponding O_3-O_4 distances, the values reveal that the oxygen−oxygen interatomic distance is smaller (2.606 Å) in model **IV** than for the less-conjugated model **I** (2.621 Å). The decrease in the distance facilitates the hydrogen transfer reaction in the larger systems. These observations suggest that the backbone conjugation helps to stabilize the system during the hydrogen-atom transfer process by reducing the charge buildup on the hydrogen atom and the two oxygen atoms involved in the IHT process. Previous studies have shown that the IHT barrier in the ground and excited states decreases linearly with respect to the oxygen−oxygen distance,[13] and that more conjugated systems exhibit a lower reaction barrier.[44]

In the $^1\pi\pi^*$ excited state, the IHT barrier becomes lower compared to the ground state. This decrease in IHT barrier, along with a strengthening of the hydrogen-bond (the O_3-H_9 distance decreases; namely, the longer O−H distance becomes shorter), has been observed previously in other model systems including malonaldehyde.[33,45] The attachment/detachment electronic densities[46] corresponding to the $^1\pi\pi^*$ excitation in models **I** and **IV** are provided in Figure 3, where the π bonding to antibonding transition is very clear. Projected density of states plots confirm that indeed the $^1\pi\pi^*$ excitation does not involve charge redistribution between the core atoms and the rest of the molecule. Therefore the transition state at the electronic excited

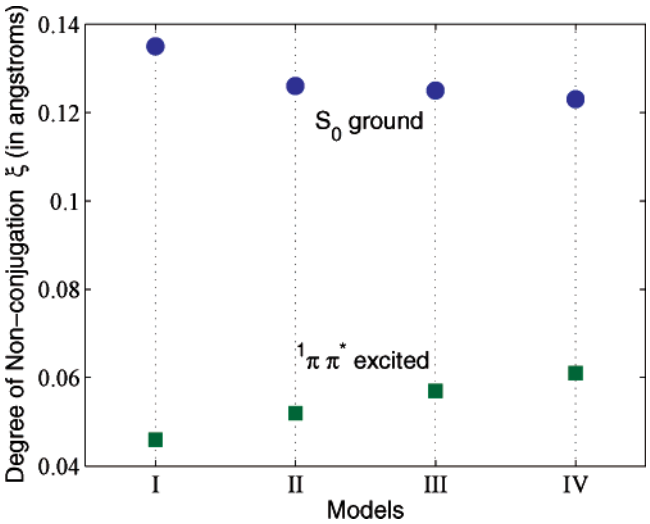

Figure 2. Nonconjugation coefficients computed at the HF/6-31++G(d,p) and CIS/6-31++G(d,p) levels of theory for models **I**−**IV** in the ground state (circles) and $^1\pi\pi^*$ excited state (squares). The plot shows that the systems become more core-conjugated in the excited state with respect to the ground state. Increase in core conjugation causes a lowering in the IHT barrier.

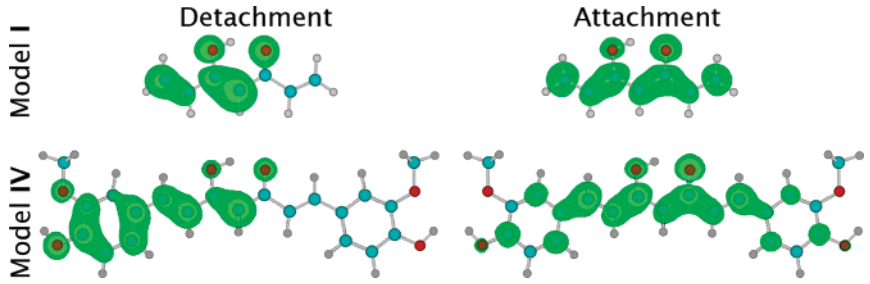

Figure 3. Electron attachment and detachment density plots involved in the $^1\pi\pi^*$ electronic excitation in models **I** and **IV**. This electronic transition corresponds predominantly to a HOMO−LUMO excitation and results in a symmetrically delocalized electron density across the enol system. As expected, the electronic excitation energy is lower in the larger systems. The excitation energy decreases from 4.70 eV in model **I** to 3.76 eV in model **IV** as calculated at the CIS/6-31++G(d,p) level of theory.

TABLE 3: Generalized Nonconjugation Coefficient ξ (Å) for Each of the Models in Figure 1[a]

	ground		excited	
	enol	TS	enol	TS
	6-31++G(d,p) Basis Set			
I	0.135	0.075	0.046	0.001
II	0.126	0.068	0.052	0.003
III	0.125	0.068	0.057	0.008
IV	0.123	0.066	0.061	0.011
	6-31G(d) Basis Set			
I	0.137	0.076	0.043	0.001
II	0.129	0.069	0.051	0.004
III	0.128	0.069	0.056	0.007
IV	0.126	0.067	0.061	0.011

[a] The different basis sets show nearly identical results. A smaller value of ξ represents a more conjugated system as the variance in the C−C bond lengths is smaller. The results show that the degree of conjugation increases in the excited state. Also observed that the conjugation dependence on the molecule size is different for the electronic state and for the transition state.

state is not stabilized by a transfer of charge. However, as observed in the plots the enol form introduces a localization effect on the nature of the π bonding of the HOMO, where a bias toward the enol side of the molecule is evident. The HOMO contributes the most to the detachment density which is plotted in Figure 3. The π^* orbital on the other hand, which compromises the most of the attached density, is shown to be symmetrically delocalized across the carbon backbone. This is the case for all the models considered. We now turn to focus on the effect this excitation has on the degree of conjugation of the system.

To obtain further physical insight into the nature of the IHT process and its dependence on conjugation, we consider, now, the generalized nonconjugation ξ coefficient as described in the previous section. A smaller value of ξ represents a more conjugated core system. As expected, we observe that the conjugation of the system increases in the ground state with an increase in the size of the backbone. This is shown in Table 3 and Figure 2 where $\xi = 0.135$ Å and 0.123 Å for models **I** and **IV**, respectively. Moreover, when the difference between the two oxygen-carbon bond lengths (C_1-O_4 and C_2-O_3) is considered, a decrease from 0.0836 Å in model **I** to 0.0808 Å in model **IV** is observed. This change therefore emphasizes the connection between higher core conjugation and lower ground state IHT barrier. Assuming that conjugation indeed stabilizes the transition state, the decrease in the ground state IHT barrier in larger systems is explained by the decrease in the nonconjugation coefficient along with the equalization of the carbon-oxygen bond lengths. We next consider the nonconjugation parameter at the electronic excited state.

An important observation is that the overall conjugation of the system is larger in the $^1\pi\pi^*$ excited state compared to the ground state. This is a consequence of the nature of the excitation as expressed by the plotted densities in Figure 3. It is found that the biased π bonding toward the enol group is delocalized across both parts of the molecule in the π^* density. This explains the large drop of the nonconjugation parameter upon the electronic excitation. For example, in model **I** the nonconjugation coefficient in the ground state (ξ) equals 0.135 Å and in the excited state $\xi = 0.046$ Å, indicating the increase in the core conjugation in the excited state. This results in the decrease of the reaction energy barrier upon excitation.

A related geometrical feature is revealed when the C_1-O_4 and C_2-O_3 distances are considered. The difference between these two distances decreases from 0.097 Å in the ground state to 0.057 Å in the excited state. Most importantly, the non-core conjugation coefficients increase for the larger systems in the excited state. This suggests that the larger systems, which are more conjugated in the ground state, become less core-conjugated than the smaller systems upon $^1\pi\pi^*$ excitation. Thus the reaction barrier for smaller systems is lower compared to larger systems in the excited state.

We now focus on the effect of backbone conjugation on the proton transfer process, at the excited state level. In a previous study, in a model where an aromatic ring is directly part of the IHT core (oHBA molecule in Figure 4), a decrease in IHT barrier upon excitation is associated with a *decrease* in the aromaticity of the considered molecule.[13] We note that this is actually still consistent with our observations above, where, however, the decrease of the core conjugation leads to increase of the reaction barrier. Our studies as outlined above show that an *increase* in the size of the coupled conjugated backbone leads to an *increase* of the reaction barrier at the excited state, whereas we find that the backbone conjugation in our models is changing only slightly. Namely, it is found that the increased core conjugation upon the excitation is reduced due to the enhanced delocalization when a larger backbone is attached to the core.

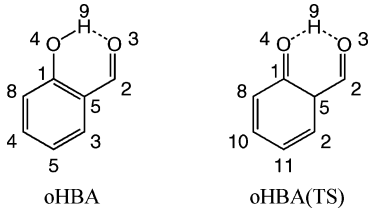

Figure 4. Molecular structure of *o*-hydroxybenzaldehyde (oHBA) in its enol and transition state (TS) configurations.

In this regard, we have first examined the aromaticity in the oHBA molecule using the same computational tools as described above and have confirmed the decrease in the aromaticity of the benzene ring in the transition state oHBA(TS) compared to the enol form. We found that the nonaromaticity parameter corresponding to the coupled benzene ring bonds increases from $\xi_{ring} = 0.029$ Å in the enol form to 0.075 Å in the transition state, confirming the decrease in aromaticity at the excited state. We comment that these are bigger changes than observed on the backbone conjugation of the model systems considered in our study above. However, more importantly, *we find that also for this system, as in the above considered model systems, the core conjugation actually increases in the transition state with respect to the enol form* ($\xi = 0.063$ Å in enol reduces to 0.034 Å in the TS). We have also analyzed the oHBA geometries reported in the study by Aquino et al.,[14] where the time-dependent DFT method was employed, and observe that in the $^1\pi\pi^*$ state, the core conjugation increases with respect to the ground state. Previous spectroscopic studies suggest that indeed an increase in conjugation leads to a lower IHT barrier in oHBA.[47] Namely, *in all considered systems the core conjugation actually increases in the transition state with respect to the enol form at the electronic excited state*. Therefore, the increase of the core conjugation at the excited state is underlying the decrease of the reaction barrier in this $^1\pi\pi^*$ excited state.

IV. Summary and Conclusion

The intramolecular hydrogen transfer barriers for various model molecules have been determined using Hartree−Fock and CIS methods. The results show that in the ground state the hydrogen transfer barrier is lower for larger systems. At the ground state, the backbone conjugation helps to lower the IHT barrier by stabilizing the transition state. However, this trend is reversed in the $^1\pi\pi^*$ excited state where the barrier increases with the increase of the conjugated backbone. The $^1\pi\pi^*$ excitation is not associated with a redistribution of charge between the core and the coupled backbone. However, this excitation leads to enhanced delocalization across the core region. This delocalization effect results in reducing the enhanced core conjugation upon excitation when a larger conjugated-backbone is coupled to the core. We observe, therefore, that upon excitation the core conjugation increases and the transition state is further stabilized leading to a lowered overall reaction barrier in comparison to the ground state. We find, in addition, that the increase of the core conjugation at the excited state is reduced with a larger coupled backbone. This results in an increase of the reaction energy barrier for models with the larger backbone at the excited electronic state level. We finally note that although the reaction energy-barrier dependence on the extent of the conjugation are quantitatively small, a valuable insight on the nature of the hydrogen-atom transfer process is revealed by considering these trends.

Acknowledgment. We thank Dr. Kevin Kubarych and Alexander Prociuk for the insightful discussions. B.D.D. acknowledges the University of Michigan for support.

References and Notes

(1) Rossetti, R.; Rayford, R.; Haddon, R. C.; Brus, L. E. *J. Am. Chem. Soc.* **1981**, *103*, 4303−4307.

(2) Barbara, P. F.; Walsh, P. K.; Brus, L. E. *J. Phys. Chem.* **1989**, *93*, 29−34.

(3) Schwartz, B. J.; Peteanu, L. A.; Harris, C. B. *J. Phys. Chem.* **1992**, *96*, 3591−3598.

(4) Sekikawa, T.; Kobayashi, T.; Inabe, T. *J. Phys. Chem. B* **1997**, *101*, 10645−10652.

(5) Grabowska, A.; Mordzinski, A.; Tamai, N.; Yoshihara, K. *Chem. Phys. Lett.* **1988**, *153*, 389−392.

(6) Douhal, A.; Lahmani, F.; Zehnacker-Rentien, A.; Amat-Guerri, F. *J. Phys. Chem.* **1994**, *98*, 12198−12205.

(7) Felker, P. M.; Lambert, W. R.; Zewail, A. H. *J. Chem. Phys.* **1982**, *77*, 1603−1605.

(8) Lochbrunner, S.; Wurzer, A.; Riedle, E. *J. Phys. Chem. A* **2003**, *107*, 10580−10590.

(9) Stock, K.; Bizjak, T.; Lochbrunner, S. *Chem. Phys. Lett.* **2002**, *354*, 409−416.

(10) Lukeman, M.; Wan, P. *J. Am. Chem. Soc.* **2002**, *124*, 9458−9464.

(11) Rios, M.; Rios, M. *J. Phys. Chem. A* **1998**, *102*, 1560−1567.

(12) Scheiner, S.; Kar, T.; Cuma, M. *J. Phys. Chem. A* **1997**, *101*, 5901−5909.

(13) Scheiner, S. *J. Phys. Chem. A* **2000**, *104*, 5898−5909.

(14) Aquino, A.; Lischka, H.; Hattig, C. *J. Phys. Chem. A* **2005**, *109*, 3201−3208.

(15) Sobolewski, A. L.; Domcke, W. *Chem. Phys.* **1994**, *184*, 115−124.

(16) Vener, M. V.; Scheiner, S. *J. Phys. Chem.* **1995**, *99*, 642−649.

(17) Zgierski, M. Z.; Fernandez-Ramos, A.; Grabowska, A. *J. Chem. Phys.* **2002**, *116*, 7486−7494.

(18) Palomar, J.; De Paz, J.; Catalan, J. *J. Phys. Chem. A* **2000**, *104*, 6453−6463.

(19) Catalan, J.; Palomar, J.; de Paz, J. *J. Phys. Chem. A* **1997**, *101*, 7914−7921.

(20) Doltsinis, N. *Mol. Phys.* **2004**, *102*, 499−506.

(21) Sharma, O. *Biochem. Pharmacol.* **1976**, *25*, 1811−2.

(22) Srivastava, KC, Bordia, A, V. S. *Leukot Essent Fatty Acids* **1995**, *52*, 223−7.

(23) Sun, Y. M.; Zhang, H. Y.; Chen, D. Z.; Liu, C. B. *Org. Lett.* **2002**, *4*, 2909−2911.

(24) Ohori, H.; Yamakoshi, H.; Tomizawa, M.; Shibuya, M.; Kakudo, Y.; Takahashi, A.; Takahashi, S.; Kato, S.; Suzuki, T.; Ishioka, C.; Iwabuchi, Y.; Shibata, H. *Mol. Cancer Ther.* **2006**, *5*, 2563−2571.

(25) Ono, K.; Hasegawa, K.; Naiki, H.; Yamada, M. *J. Neurosci. Res.* **2004**, *75*, 742−750.

(26) Yang, F.; Lim, G. P.; Begum, A. N.; Ubeda, O. J.; Simmons, M. R.; Ambegaokar, S. S.; Chen, P. P.; Kayed, R.; Glabe, C. G.; Frautschy, S. A.; Cole, G. M. *J. Biol. Chem.* **2005**, *280*, 5892−5901.

(27) Jovanovic, S.; Steenken, S.; Boone, C.; Simic, M. *J. Am. Chem. Soc.* **1999**, *121*, 9677−9681.

(28) Balasubramanian, K. *J. Agric. Food Chem.* **2006**, *54*, 3512−20.

(29) Jonas, D. M. *Annu. Rev. Phys. Chem.* **2003**, *54*, 425−463.

(30) Khalil, M.; Demirdoven, N.; Tokmakoff, A. *J. Phys. Chem. A* **2003**, *107*, 5258−5279.

(31) Kolano, C.; Helbing, J.; Kozinski, M.; Sander, W.; Hamm, P. *Nature* **2006**, *444*, 469−72.

(32) Latajka, Z.; Scheiner, S. *J. Phys. Chem.* **1992**, *96*, 9764−9767.

(33) Luth, K.; Scheiner, S. *J. Phys. Chem.* **1994**, *98*, 3582−3587.

(34) Arias, A. A.; Wasserman, T. A. W.; Vaccaro, P. H. *J. Chem. Phys.* **1997**, *107*, 5617−5620.

(35) Barone, V.; Adamo, C. *J. Chem. Phys.* **1996**, *105*, 11007−11019.

(36) Becke, A. D. *J. Chem. Phys.* **1993**, *98*, 5648−5652.

(37) Lee, C.; Yang, W.; Parr, R. G. *Phys. Rev. B* **1988**, *37*, 785−789.

(38) Kolev, T. M.; Velcheva, E. A.; Stamboliyska, B. A.; Spiteller, M. *Int. J. Quantum Chem.* **2005**, *102*, 1069−1079.

(39) Foresman, J. B.; Head-Gordon, M.; Pople, J. A.; Frisch, M. J. *J. Phys. Chem.* **1992**, *96*, 135−149.

(40) Shao, Y.; *et al. Phys. Chem. Chem. Phys.* **2006**, *8*, 3172−91.

(41) Lopez Sancho, M. P.; Lopez Sancho, J. M.; Rubio, J. *J. Phys. F: Met. Phys.* **1985**, *15*, 851−858.

(42) Kong, L.; Priyadarsini, K. I.; Zhang, H. Y. *J. Mol. Struct. (THEOCHEM)* **2004**, *684*, 111−116.

(43) Latajka, Z.; Bouteiller, Y.; Scheiner, S. *Chem. Phys. Lett.* **1995**, *234*, 159−164.

(44) Wang, D.-P.; Chen, S.-G.; Chen, D.-Z. *J. Photochem. Photobiol. A: Chem.* **2004**, *162*, 407−414.

(45) Chen, D.-Z.; Wang, D.-P.; Zhang, H.-Y.; Tang, B. *Chem. Phys. Lett.* **2002**, *353*, 119−126.

(46) Head-Gordon, M.; Grana, A. M.; Maurice, D.; White, C. A. *J. Phys. Chem.* **1995**, *99*, 14261−14270.

(47) Morgan, M. A.; Orton, E.; Pimentel, G. C. *J. Phys. Chem.* **1990**, *94*, 7927−7935.